# Structural Flexibility in Hydrated Proteins

**Stephen Bone***

*Institute for Bioelectronic and Molecular Microsystems, Bangor University, Dean Street, Bangor LL571UT, Gwynedd, U.K.*

*Received: February 1, 2008; Revised Manuscript Received: May 16, 2008*

The flexibility of protein structures is important in allowing the variety of motions, covering a wide range of magnitudes and frequencies, essential to biological activity. Protein flexibility is also implicated in denaturation, allowing proteins to take up nonactive comformations that have free energies close to that of the native state. High-frequency dielectric measurement can be used to study the flexibility of proteins by probing the relaxation of dipolar constituents of their structures. In this work, 14 hydrated globular proteins are investigated using this method. Four relaxation processes are identified, one of which, with a relaxation time of 19 ns, can be correlated with the sum of the number densities of protein glycine and alanine residues. A second with a relaxation time of 2 ns shows a dependence on the number of threonine residues. It is concluded that the dipolar peptide groups of the protein backbone associated with these residues are responsible for these dielectric responses, with the lower frequency dispersion being due to backbone mobility in the hydrophobic environment of the protein core and the higher frequency response being associated with mobility on the more hydrophilic protein surface. The correlation of protein backbone flexibility with particular side chains indicates that these protein motions are under the direct control of the amino acid sequence of the protein.

## Introduction

The scale of protein internal motion in terms of amplitude, energy, and time vary over many orders of magnitude, indicating a range of possible individual, collective, and cooperative types of motions. For instance, small, closely packed groups of atoms may experience very short time, with small amplitude motions on the order of $10^{-13}$ s and 0.02 nm. In less closely packed regions of the protein, much larger displacements may occur, possibly involving the partial unfolding of a region of the protein. The types of motion involved may include rotational orientation of groups about individual bonds, the concerted movement of a number of side chains or section of the main peptide chain relative to the rest of the protein structure, or the fluctuating motion of counterions or solvent molecules associated with the protein.[1] In order to access these structural motions, the protein must exhibit flexibility in that part of the structure. Flexibility in proteins is an important determinant in biological functionality. Many enzymatic reactions involve considerable conformational changes in the protein and the associated substrate.[2] However, structural flexibility may also lead to instability, unfolding, and the adoption of inactive structures since there are a large number of conformations with free energies close to that of the native state. In fact, some protein preservatives are thought to act through their ability to limit structural motions that are associated with denaturing transitions.[3] In the native state, protein flexibility is moderated by steric hindrances, hydrophobic interactions, and electrostatic interactions, for example, salt bridges.[4] Importantly, electrostatic interactions are themselves modified by water molecules, clusters of which are found on the protein surface [5–8] and occasionally in the protein interior.[9–12]

Dielectric measurements over the frequency range of 1 MHz to 20 GHz are well suited to the investigation of protein structural flexibility, being able to probe dipolar components and obtain values of effective dipole moments. In this work, 14 hydrated globular proteins are studied, and their dielectric characteristics are correlated with structural components.

## Experimental Methods

**Theoretical.** For dipolar orientational relaxation in materials at low levels of hydration, the Onsager correction for local electric field is relevant. The corrected magnitude of the dielectric dispersion, $F(\varepsilon)$, as developed by Kirkwood, Fröhlich, and others is given by[13]

$$F(\varepsilon) = \frac{(\varepsilon_s - \varepsilon_\infty)(2\varepsilon_s + \varepsilon_\infty)}{\varepsilon_s(\varepsilon_\infty + 2)^2} = \frac{Ng\langle\overline{\mu}\rangle^2}{9\varepsilon_0 kT} \quad (1)$$

where $\varepsilon_s$ and $\varepsilon_\infty$ are the limiting low and high frequency permittivity values of each dispersion, and $\varepsilon_0$ is the permittivity of free space. $N$ is the number density of dipoles, $\langle\mu\rangle$ is the mean effective dipole moment, and the Kirkwood correlation factor, $g$, accounts for correlated dipole motion ($g \geq 1$ and has a value of unity for uncorrelated dipoles).

The characteristic relaxation time, $\tau$, as derived by Eyring, is given by

$$\tau = \frac{1}{2\pi f} = \frac{h}{kT}\exp\left(\frac{\Delta G}{RT}\right) = \frac{h}{kT}\exp\left(-\frac{\Delta S}{R}\right)\exp\left(\frac{\Delta H}{RT}\right) \quad (2)$$

where $f$ is the relaxation frequency, and $\Delta G$, $\Delta H$, and $\Delta S$ are the activation free energy, enthalpy, and entropy of the relaxation process, respectively.

The dielectric permittivity and loss characteristics were modeled using a superposition of dispersions, each represented by $J_k(\omega)$ where the complex permittivity $\varepsilon^*$ is given by

$$\varepsilon^*(\omega) = \varepsilon'(\omega) - i\varepsilon''(\omega) = \varepsilon_\infty + \sum_{k=1}^{k} J_k(\omega) \quad (3)$$

If the relaxation time and magnitude of each dispersion is denoted by $\tau_k$ and $M_k$, then

* E-mail address: s.bone@.bangor.ac.uk.

10.1021/jp8009782 CCC: $40.75 
Published on Web 07/23/2008

$$J_k(\omega) = \frac{M_k}{1 + (i\omega\tau_k)^{1-\alpha}} \quad (4)$$

where α is included to account for a distribution of relaxation times ($0 \leq \alpha \leq 1$).

## Materials and Methods

All proteins were purchased from Sigma Chemical Company and were used without further treatment as follows: bovine serum albumen fraction V, lysozyme from chicken egg white (3× crystallized, dialyzed, and lyophilized), pepsin from porcine stomach mucosa, catalase from bovine liver, β-lactoglobulin from bovine milk (3× crystallized and lyophilized), hexokinase from bakers yeast, casein from bovine milk, trypsin inhibitor from soybean, chymotrypsinogen A from bovine pancreas, glucose oxidase from *Aspergillus niger*, lipase from *Candida cylindracea,* urease type III from jack beans, ribonuclease A from bovine pancreas, and hemoglobin, lyophilized from bovine blood.

Dielectric measurements over the frequency range of 1 MHz to approximately 20 GHz were performed using a technique known as time-domain reflectometry (TDR). In a typical TDR experiment, a train of voltage steps of magnitude 500 mV and risetime 25 ps is transmitted from a tunnel diode down a low-loss coaxial line terminated by air-line containing the sample. In the particular method used (the precision difference method),[14] the reflected voltage waveform from the sample is compared with that from a reference dielectric of known complex permittivity. By using the appropriate time windows and sample cell lengths and after suitable transformation from time- to frequency-domain, it is possible to accurately determine the dielectric characteristics of the sample. For the frequency range 1 MHz to 1 GHz, data was analyzed over a 140 ns time window using a coaxial sample cell length of 5 mm with inner and outer electrode diameters 5 mm and 7 mm, respectively. For frequencies between 0.5 GHz and 20 GHz, a time window of 5 ns and effective cell length of 0.2 mm were employed. A digital storage oscilloscope (Hewlett-Packard 54120A) with a four-channel test set (HP 54121A), which includes a dedicated TDR test port, was employed for data capture.

For hydration measurements, protein samples of density $1.5-9.5 \times 10^5$ g m$^{-3}$ were exposed to hydration levels over the range of 0−85% relative humidity (RH), where 0% was considered to be the state reached after the sample had been in equilibrium with a vacuum of $1 \times 10^{-2}$ mbar for 24 h. Water partial pressures were measured using a Honeywell humidity sensor (typeHIH-3610), which had been previously calibrated using saturated salt solutions. Hydration isotherms of proteins were produced using a Sartorius vacuum microbalance (type 4133).

A genetic algorithm using Matlab and the Genetic Algorithm and Direct Search Toolbox was employed to achieve the best fit of the theoretical equations (eqs 3 and 4) to the experimental data. Genetic algorithms are very effective in searching the model space and, compared to gradient search methods, are much more likely to converge toward a global minimum. Typical parameters used were as follows: number of generations, 400 000; tolerance function, $10^{-7}$; population size, 200[2]; crossover, 0.8; elite count, 4; number of games, 30.

## Results and Discussion

A typical high-frequency permittivity characteristic for a hydrated protein is shown in Figure 1. This data indicates the presence of a number of relaxation processes with relaxation times extending over the range of 10 ps to 100 ns. These can be identified more easily from Figure 2, which shows the corresponding experimentally determined dielectric loss and constituent dispersions obtained from modeling using equations 3 and 4 in conjunction with a genetic algorithm program (Matlab). Table 1 gives details of the dielectric parameters of each of the component dispersions used to fit the experimental data together with the associated modeling error. Three relaxation processes, designated I to III, were unambiguously identified together with a fourth dispersion, which exhibited a

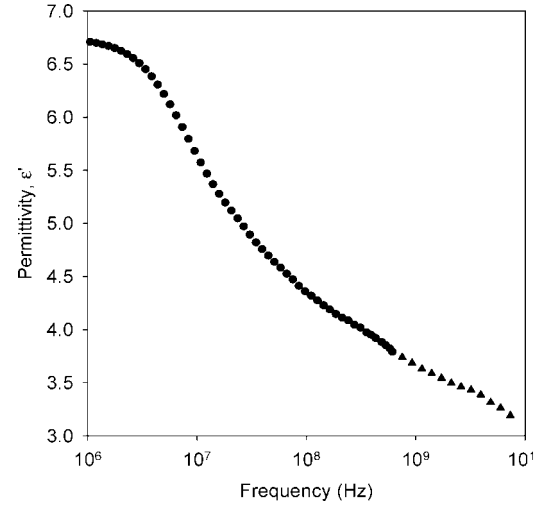


**Figure 1.** High-frequency dielectric characteristic of lysozyme; variation of the real component of the complex permittivity, ε′, with frequency at 75% RH and 298 K. Filled circles represent data collected in a 140 ns time window for a coaxial sample cell length of 20 mm (inner and outer electrode diameters 5 mm and 7 mm, respectively) and filled triangles indicate a 5 ns time window and effective cell length of 1.04 mm.

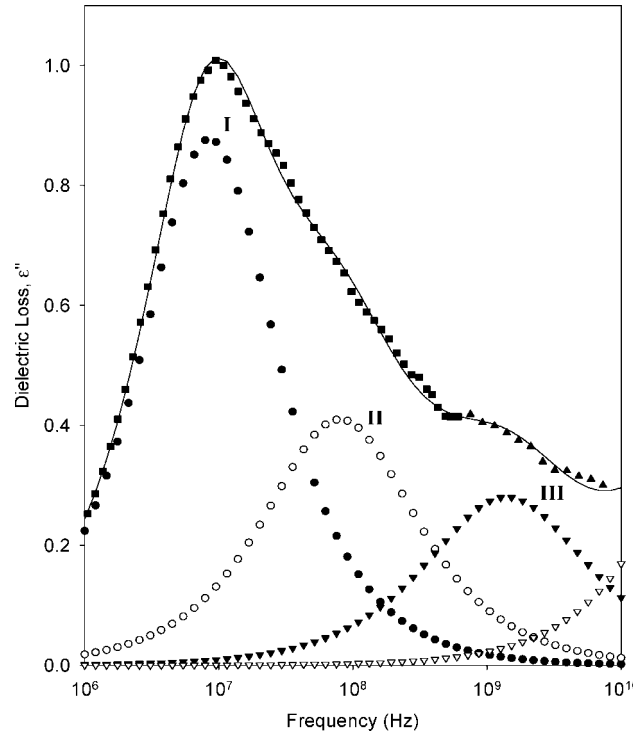


**Figure 2.** High-frequency dielectric characteristic of lysozyme; variation of the imaginary component of the complex permittivity, ε″, with frequency at 75% RH and 298 K. The solid line is the sum of the individual components. Experimental details are identical to those of Figure 1.

**TABLE 1: Dielectric Parameters of Component Dispersions for Lysozyme at 75% RH and 298 K[a]**

| | dispersion I | dispersion II | dispersion III | dispersion IV |
|---|---|---|---|---|
| $\varepsilon_s$ | 6.75 ± 0.04 | 4.91 ± 0.03 | 3.95 ± 0.02 | 3.22 ± 0.1 |
| $\varepsilon_i$ | 4.91 ± 0.04 | 3.95 ± 0.03 | 3.22 ± 0.02 | 2.22 ± 0.1 |
| $M$ | 1.84 ± 0.06 | 0.96 ± 0.04 | 0.62 ± 0.03 | 1.04 ± 0.14 |
| $\tau$ (ns) | 18.7 ± 0.4 | 2.0 ± 0.1 | 0.11 ± 0.01 | 0.003 ± 0.001 |
| α | 0.08 ± 0.01 | 0.10 ± 0.03 | 0.14 ± 0.03 | 0.09 ± 0.01 |

[a] Errors are given as ±1 s.

relaxation frequency above the technical limits of the TDR measurement system. Adoption of a larger number of dispersions in the modeling process produced multiple dispersions with very similar relaxation frequencies and fewer dispersions resulted in unrealistically large values of α. Dispersions I and II could be relatively accurately characterized, while dispersions III and IV were subject to significantly larger experimental and modeling errors.

This work describes the hydration dependence of dispersions I and II and considers correlation of the experimental data with protein composition. An indication of the error associated with these dispersions was obtained from 10 repeat experiments on lysozyme and on serum albumen with RHs raised to 80% before each measurement (298 K). For dispersion I, which was dominant in all proteins, results indicated standard deviations of the magnitude and relaxation frequency of ± 5% and ± 4%, respectively. The smaller dispersion II was subject to greater error, with standard deviations of ± 9% and ± 8%, respectively, for the same dielectric parameters.

The high-frequency dielectric characteristics of 14 proteins were measured at RHs of 70 and 80%. In addition, relaxation measurements were made on two proteins, chymotrypsin and hemoglobin, over the range of hydrations 0 to 90% RH. Absorption isotherms, detailing the amount of bound water at these RHs, were also determined. Values of the relaxation time $\tau$ and distribution parameter α for dispersions I and II were found to be constant with hydration within experimental error. However, the dispersion magnitude $M$ and related parameters exhibited significant hydration dependence. Dispersion I data in the form of $F(\varepsilon)$ (eq 1), normalized for differences in sample density, is plotted against protein water content (%w/w) in Figure 3. This clearly shows two different characteristics to which all 14 proteins (with the possible exception of glucose oxidase) adhere. $F(\varepsilon)$ rises relatively slowly with increasing water content at low hydration levels in both characteristics and in the lower response, the rate of increase at higher levels is only slight. In contrast, the upper characteristic shows a rapid rate of increase with increasing hydration. Hydration-induced increases in protein structural mobility have been previously reported and are consistent with a scheme in which water reduces the potential barrier associated with the relaxation process.[5–7] Water molecules are engaged in single and multiple hydrogen bonding to the protein. Importantly, a proportion of these are rotationally mobile and therefore polarizable. This produces relatively high local permittivities and effective screening of inter- and intramolecular electrostatic interactions between polar species resulting in significant flexibility of the protein structure.

Hydrated proteins have been considered to possess sufficient complexity to exhibit the type of cooperative dynamic motion found in some glass-forming polymer systems. However, a well defined change in heat capacity at a specific glass transition temperature, observed for linear polymers,[15] is not found for proteins; instead a more gradual smeared out change over a

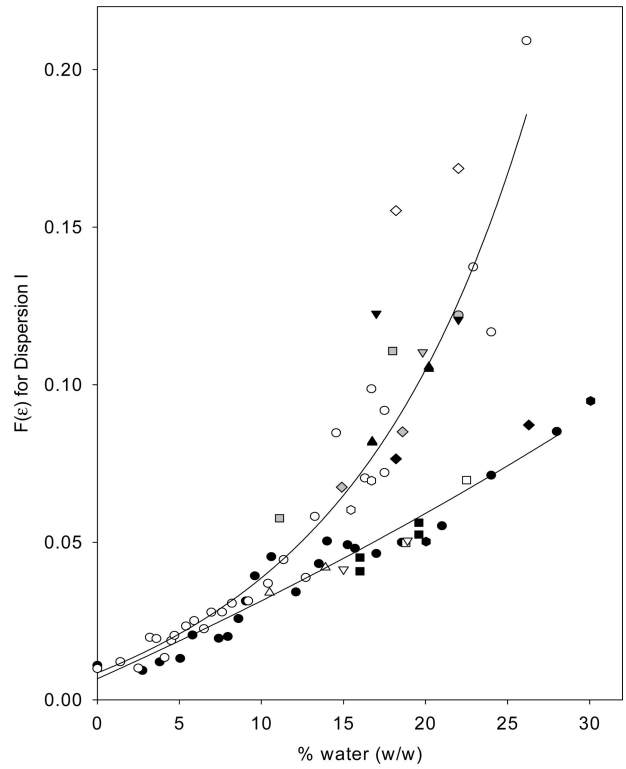


**Figure 3.** Dependence of dielectric parameter $F(\varepsilon)$ for dispersion I on hydration level at 298 K. ● hemoglobin, ○ chymotrypsin, ▲ lysozyme, ■ bovine serum albumin, △ casein, ⬡ pepsin, (gray ◇) chymotrypsinogen, ◆ glucose oxidase, ⬢ β-lactoglobulin, ▼ hexokinase, (gray ▽) catalase, (gray □) lipase, (gray ○) trypsin inhibitor, ▽ hemoglobin, □ ribonuclease, ◇ urease.

temperature range is seen.[16–18] It is tempting to associate the rapid rise in the magnitude of the dielectric parameter $F(\varepsilon)$ shown in the upper characteristic in Figure 3 with increasing flexibility of the protein structures. In this case, increasing the water content of the protein lowers the glass transition temperature below the measurement temperature, allowing protein structural mobility to be observed. The reason for the bimodal nature of the protein data is not clear but interestingly all proteins that form the higher characteristic, except trypsin inhibitor, are enzymes, while ribonuclease is the only enzyme in the group of proteins forming the lower characteristic. The fact that all of the proteins studied adhere to the two curves in Figure 3 indicates the existence of common dynamic mechanisms.

Use of the data set from all studied proteins allowed results to be analyzed for possible correlation with protein structural components. Amino acid sequences for the proteins studied were obtained from the Swiss-Prot/TrEMBL protein knowledgebase.[19] In the case of dispersion I, a correlation is found between $F(\varepsilon)$ and the sum of the number densities of glycine and alanine side chains, as shown in Figure 4. It should be noted that the $F(\varepsilon)$ value for each protein at a constant RH (70%), rather than at a specific water content, is plotted, so that to a first approximation it can be assumed that identical structural components in different proteins are hydrated to the same extent. It is clear that, since glycine and alanine side chains are nonpolar, dispersion I cannot be directly associated with the relaxation of these groups. It is more likely that the polar peptide units of the protein backbone to which these groups are bound are the relaxing species, the small side chains (−H and $-CH_3$) associated with these amino acids, allowing peptide group mobility. It is known that, while the peptide group itself is relatively rigid, there is a significant degree of rotational freedom

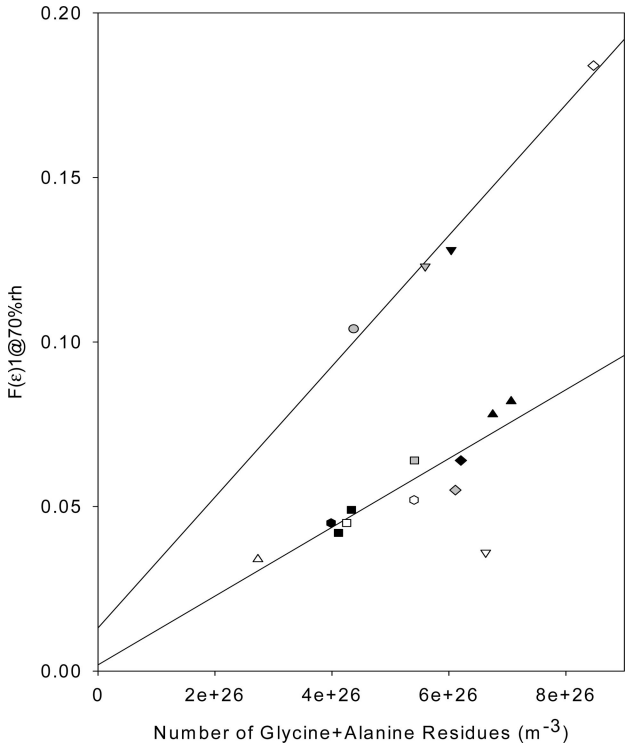


**Figure 4.** Variation of the dielectric parameter $F(\varepsilon)$ of dispersion I at 298 K and 70% RH with the sum of the concentrations of glycine and alanine residues. ▲ lysozyme, ■ bovine serum albumin, △ casein, ⬡ pepsin, (gray ◇) chymotrypsinogen, ◆ glucose oxidase, ⬢ $\beta$-lactoglobulin, ▼ hexokinase, (gray ▽) catalase, (gray □) lipase, (gray ○) trypsin inhibitor, ▽ hemoglobin, ◇ urease.

**TABLE 2: Effective Dipole Moments**[a]

| dispersion/ hydration | dipole moment (lower) | dipole moment (higher) |
|---|---|---|
| dispersion I 70% RH | $5.87 \times 10^{-30}$ cm (1.76 D) | $8.08 \times 10^{-30}$ cm (2.42 D) |
| dispersion I 80% RH | $6.95 \times 10^{-30}$ cm (2.08 D) | $8.41 \times 10^{-30}$ cm (2.52 D) |
| dispersion II 70% RH | $8.2 \times 10^{-30}$ cm (2.46 D) | $11.4 \times 10^{-30}$ cm (3.41 D) |
| dispersion II 80% RH | $9.3 \times 10^{-30}$ cm (2.78 D) | $14.4 \times 10^{-30}$ cm (4.31 D) |

[a] Calculated assuming $g = 1$ (eq 1).

about the bonds either side. Given the difference in size and rotational mobility of glycine and alanine as described by their Ramachandran plots, a larger distribution of relaxation times for the backbone motions of dispersion I might have been expected. However, this dependence is consistent with NMR studies on urea-denatured apomyoglobin, where glycine and alanine residues were found to result in increased backbone flexibility[20] and also with studies on serpins and viral fusion peptides where the prevalence of glycine and alanine were linked to mobile reactive center loops.[21] The calculated dipole moments associated with the two slopes are $5.9 \times 10^{-30}$ cm (1.8 D) and $8.1 \times 10^{-30}$ cm (2.4 D) compared with the dipole moment of an unhindered peptide bond of ~3.7 D units. It is likely that the two linear plots of Figure 4 and calculated dipole moments represent proteins that are below and above the glass transition, respectively, at 298 K and 70% RH. The characteristics at 80% RH (not shown) are similar except for the fact that $\beta$-lactoglobulin is promoted to the upper line, indicating that it goes through a glass transition between the two hydrations levels. The calculated values for the mean effective dipole moments of the peptide groups for dispersion I are shown in Table 2. The data point for hemoglobin in Figure 4 is a significant outlier and was omitted from the least-squares fitting (LSF) procedure.

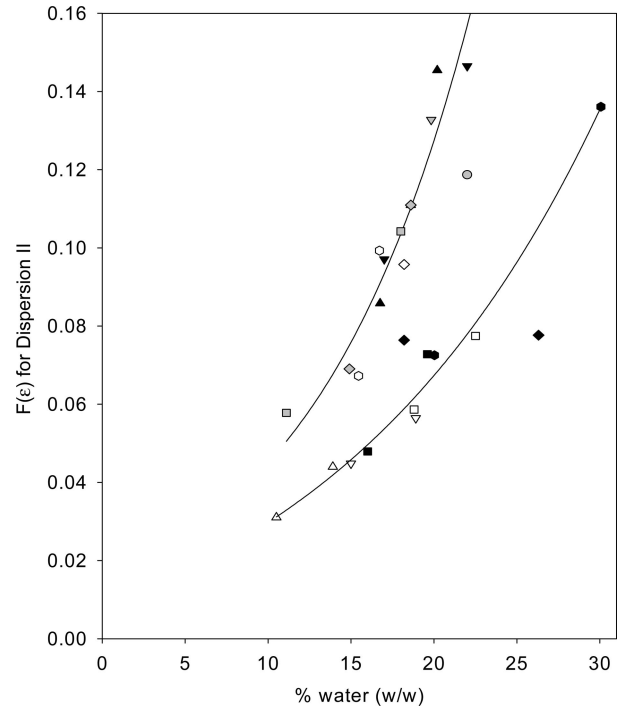


**Figure 5.** Dependence of dielectric parameter $F(\varepsilon)$ for dispersion II on protein water content at 298 K. ▲ lysozyme, ■ bovine serum albumin, △ casein, ⬡ pepsin, (gray ◇) chymotrypsinogen, ◆ glucose oxidase, ⬢ $\beta$-lactoglobulin, ▼ hexokinase, (gray ▽) catalase, (gray □) lipase, (gray ○) trypsin inhibitor, ▽ hemoglobin, ◇ urease.

The fit of upper and lower lines to the data points is characterized by $r^2$ values of 0.98 and 0.87, respectively.

The fact that the magnitude of $F(\varepsilon)$ of dispersion I is dependent on protein water content (Figure 3) indicates one of two possibilities. Either water is able to penetrate the protein core and bind to the peptide bonds associated with the relaxation mechanism, or water bound to the protein surface influences, at a distance or by cooperative motions, the peptide group relaxations. If the former is the case, this implies that, in hydrated proteins, the protein core is much less compact compared with the protein in solution where the packing density of hydrophobic core is such that water incursion is a relatively rare unless a structural cavity exists where water can be hydrogen bonded in a thermodynamically stable and long-lived manner.[11,12]

A similar bimodal characteristic to that encountered for dispersion I is evident in Figure 5 where $F(\varepsilon)$ for dispersion II, normalized for sample density, is plotted against the percentage of protein water content at 70% and 80% RH. The proteins studied are clearly divided into two groups, with the same proteins present in the upper and lower responses as were found in the characteristics for dispersion I. In this case, both characteristics rise in an exponential way with increasing protein water content, indicating a hydration-dependent mobility. The data has been analyzed for possible dependence on the amino acid composition of each protein. An apparent correlation is described in Figure 6, where $F(\varepsilon)$ for dispersion II at 80% RH is plotted against the number density of threonine residues in each protein sample. A linear dependence is evident, particularly for proteins lying on the lower line. The LSF of the upper and lower lines is characterized by $r^2$ values of 0.91 and 0.92, respectively. Although this side chain has been implicated in a number of studies in the facilitation of protein backbone flexibility,[22–25] it is not clear why threonine residues specifically

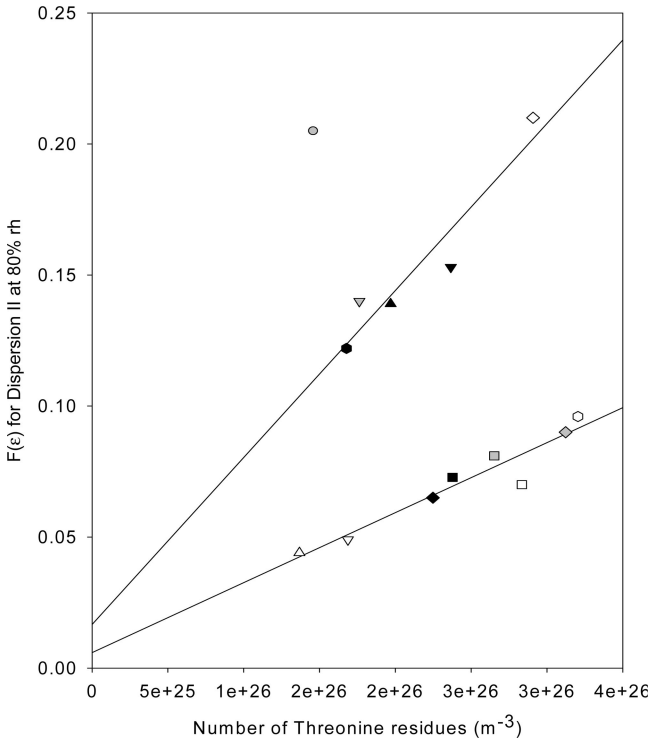


**Figure 6.** Variation of the dielectric parameter $F(\varepsilon)$ of dispersion II at 298 K and 80% RH with the sum of the concentrations of threonine residues. ▲ lysozyme, ■ bovine serum albumin, △ casein, ⬡ pepsin, (gray ◇) chymotrypsinogen, ◆ glucose oxidase, ⬢ $\beta$-lactoglobulin, ▼ hexokinase, (gray ▽) catalase, (gray □) lipase, (gray ○) trypsin inhibitor, ▽ hemoglobin, ◇ urease.

should be associated with protein dynamics. As a result of its hydroxyl group, threonine will exhibit a small dipole moment. However, as with dispersion I, it is more likely that the origin of dispersion II lies in the relaxation of the peptide units of the protein backbone, which bind threonine residues. The calculated mean effective dipole moment of the peptide units associated with dispersion II are shown in Table 2. It can be seen that the effective mean dipole moment of the peptide units calculated from the upper characteristics show a relatively large increase in value from 3.4 D at 70% RH to 4.3 D at 80% RH. The latter value is in fact larger than the calculated maximum dipole moment of 3.7 D. This may be explained in terms of the onset of cooperative concerted motions of the protein backbone resulting in a correlation factor of $g > 1$ (eq 1). The data point for trypsin inhibitor is a clear outlier in Figure 6.

Both dispersions I and II are considered to originate from orientational polarization of the peptide units. However, the dielectric characteristics of these two processes are quite different. From Table 1 it can be seen that dispersion I has a relaxation time approximately 10 times longer and an effective dipole moment significantly smaller than those of dispersion II. This is consistent with a relatively compact hydrophobic environment for the relaxation of the peptide units associated with glycine and alanine residues compared with that for the protein backbone in the vicinity of threonine residues, the majority of which are expected to be found on the hydrophilic protein surface.

In conclusion, a direct correlation has been found between the high frequency permittivity of hydrated proteins and their amino acid compositions, specifically the number density of glycine, alanine, and threonine residues. The finding that the peptide unit mobility for all proteins studied appears to adhere to one of two possible schemes indicates common dynamic mechanisms. The correlation of backbone flexibility with specific side chains indicates that protein dynamics are under the direct control of the amino acid sequence.

**Acknowledgment.** I thank Professor R. Pethig for valuable discussions.

## References and Notes

(1) Gerstein, M.; Krebs, W. *Nucleic Acids Res.* **1998**, *26*, 4280–4290.
(2) Kumar, S.; Ma, B.; Tsai, C. J.; Wolfson, H.; Nussinov, R. *Cell Biochem. Biophys.* **1999**, *31*, 141–164.
(3) Lopez-Diez, E. C.; Bone, S. *Biochim. Biophys. Acta* **2004**, *1673*, 139–148.
(4) Kumar, S.; Wolfson, H. J.; Nussinov, R. *IBM J. Res. Dev.* **2001**, *45*, 499–512.
(5) Bone, S.; Pethig, R. *J. Mol. Biol.* **1982**, *157*, 571–575.
(6) Bone, S.; Pethig, R. *J. Mol. Biol.* **1985**, *181*, 323–326.
(7) Bone, S. *Biochim. Biophys. Acta* **1987**, *916*, 128–134.
(8) Bone, S. *Phys. Med. Biol.* **1996**, *41*, 1265–1275.
(9) Yu, B.; Blaber, M.; Gronenborn, A. M.; Clore, G. M.; Caspar, D. L. D. *Proc. Natl. Acad. Sci. U.S.A.* **1999**, *96*, 103–108.
(10) Sanschagrin, P. C.; Kuhn, L. A. *Protein Sci.* **1998**, *7*, 2054–2064.
(11) Pineda, A. O.; Carrell, C. J.; Bush, L. A.; Prasad, S.; Caccia, S.; Chen, Z-W.; Mathews, S.; Di Cera, E. *J. Biol. Chem.* **2004**, *279*, 31842–31853.
(12) Bone, S. *J. Phys. Chem. B* **2006**, *110* (41), 20609–20614.
(13) Hill, N. E.; Vaughan, W. E.; Price, A. H.; Davies, M. *Dielectric Properties and Molecular Behaviour*; Van Nostrand Reinhold: London, 1969.
(14) Nakamura, H.; Mashimo, S.; Wada, A. *Jpn. J. Appl. Phys.* **1982**, *21*, 467–474.
(15) Khanna, Y. P.; Kuhn, W. P.; Sichina, W. J. *Macromolecules* **1995**, *28*, 2644–2646.
(16) Sochava, I. V. *Biophys. Chem.* **1997**, *69*, 31–41.
(17) Prabhu, N. V.; Sharp, K. A. *Annu. Rev. Phys. Chem.* **2005**, *56*, 521–48.
(18) Tsereteli, G. I.; Belopolskaya, T. V.; Grunina, N. A.; Vaveliouk, O. L. *J. Therm. Anal. Calorim.* **2000**, *62*, 89–99.
(19) Swiss-Prot Protein Knowledgebase Database. http://expasy.org/sprot/.
(20) Schwartzinger, S.; Wright, P. E.; Dyson, H. J. *Biochemistry* **2002**, *41*, 12681–12686.
(21) Callebaut, I.; Tasso, A.; Brasseur, R.; Burny, A.; Portetelle, D.; Mornon, J. P. *J. Comput.-Aided Mol. Des.* **1994**, *8*, 175–191.
(22) Stites, W. E.; Pranata, J. *Proteins: Struct., Funct., Genet.* **1995**, *22* (2), 132–140.
(23) Gronwald, W.; Chao, H. M.; Reddy, D. V.; Davies, P. L.; Sykes, B. D.; Sonnichsen, F. D. *Biochemistry* **1996**, *35* (51), 16698–16704.
(24) Kantarci, N.; Tamerler, C.; Sarikaya, M.; Haliloglu, T.; Doruker, P. *Polymer* **2005**, *46* (12), 4307–4313.
(25) Poon, D. K. Y.; Withers, S. G.; McIntosh, L. P. *J. Biol. Chem.* **2007**, *282* (3), 2091–2100.

JP8009782